RSC Advances

PAPER

View Article Online
View Journal | View Issue

Cite this: *RSC Adv.*, 2017, **7**, 46938

ent-Rosane diterpenoids from *Euphorbia milii* showing an Epstein–Barr virus lytic replication assay†

Shao-Nan Liu,‡[a] Jiayuan Hu,‡[b] Shen H. Tan,[a] Qian Wang,[b] Jun Xu,[a] Yan Wang,[c] Yan Yuan*[bd] and Qiong Gu*[a]

Received 11th August 2017
Accepted 28th September 2017

DOI: 10.1039/c7ra08877a

rsc.li/rsc-advances

The phytochemical investigation on the acetone extract of *Euphorbia milii* afforded thirteen new *ent*-rosane diterpenoids (**1–13**) through bioassay guided fractionation for evaluating its effect on Epstein–Barr virus (EBV) DNA lytic replication. Structures were determined by comprehensive spectroscopic analyses including 1D & 2D NMR techniques, chemical methods, and experimental and calculated electronic circular dichroism (ECD) data. The absolute configuration of euphominoid A (**1**) was established by single crystal X-ray diffraction analysis of its *p*-bromobenzoate derivative **1a**. Compounds **1–3**, and **10** displayed inhibitory activity with EC_{50} values ranging from 5.4 to 29.1 μM and selective index (SI) values varied from 4.5 to 9.3. Compound **2** showed the most potent inhibitory activity with an EC_{50} value of 5.4 μM comparing with the positive control (+)-rutamarin (EC_{50} = 5.4 μM). This is the first report of *ent*-rosane-type diterpenoids exhibiting significant inhibition of EBV lytic replication.

Introduction

Euphorbia milii Linn. (Euphorbiaceae) is a flowering plant mainly distributed in the southwestern region of China. The *Euphorbia* genus have provided approximately 400 characteristic diterpenoids possessing a broad range of biological activities.[1–4] Several secondary metabolites isolated from the *Euphorbia* genus exhibited anti-viral activity against HIV, HSV, and Epstein–Barr virus (EBV).[5–14] This plant has been extensively used as a detoxifying agent in traditional Chinese medical (TCM) treatments.[15]

We have recently reported novel secondary metabolites from the *E. milii*,[16] during a continuing program towards the discovery of anti-viral natural products.[9,17,18] Herein, we report the detailed chemical investigation of the 80% acetone extract of the aerial parts of *E. milii*. This extract displayed inhibitory activity against EBV lytic replication with an EC_{50} value of 12.4 μg mL^{-1}. Bioactivity-guided isolation led to the isolation and identification of thirteen new *ent*-rosane diterpenoids (**1–13**), some of which exhibited promising EBV lytic replication inhibitory activity.

Results and discussion

Compound **1**, obtained as a white powder. Its HRESIMS spectrum showed the sodiated adduct ion at *m/z* 325.2132 $[M + Na]^+$ corresponding to the molecular formula of $C_{20}H_{30}O_2$. The IR signals at 3408 and 1695 cm^{-1} revealed the presence of a hydroxy group and a carbonyl group. The ^1H NMR data of compound **1** (Table 1) exhibited characteristic signals of a vinyl group [δ_H 5.79 (1H, dd, J = 17.5, 10.7 Hz), 4.90 (1H, d, J = 17.5 Hz), and 4.82 (1H, d, J = 10.7 Hz)], a hydroxymethyl group [δ_H 3.59 (1H, d, J = 11.0 Hz), 3.65 (1H, d, J = 11.0 Hz)], and three methyl singlets (δ_H 0.91, 1.00, and 1.04). The ^{13}C NMR and DEPT spectra of compound **1** showed 20 carbon resonances, comprising those of a carbonyl group at δ_C 216.5, two pairs of olefinic carbons (δ_C 129.7 and 141.3, 108.7 and 150.8), and three methyls (δ_C 16.9, 18.8, and 22.9). These data implied that the 2D structure of compound **1** is similar to that of engleromycenol,[19] except for a carbonyl group in compound **1** in place of a methylene group at C-3 in engleromycenol. The HMBC cross-peaks of H_3-18 with C-3, C-4, and C-5 (Fig. 1) confirmed a carbonyl group positioned at C-3. Thus, the 2D structure of compound **1** was established as shown.

The relative configuration of compound **1** was deduced from the NOESY spectrum (Fig. S8, ESI†). The NOESY cross-peaks of

[a]*Research Center for Drug Discovery, School of Pharmaceutical Sciences, Sun Yat-sen University, Guangzhou 510006, People's Republic of China. E-mail: guqiong@mail.sysu.edu.cn; Fax: +86-20-39943077; Tel: +86-20-39943077*

[b]*The Institute of Human Virology, Zhongshan School of Medicine, Sun Yat-sen University, Guangzhou, Guangdong 510080, People's Republic of China. E-mail: yuan2@pobox.upenn.edu*

[c]*Guanghua School of Stomatology, Sun Yat-sen University, Guangdong Provincial Key Laboratory of Stomatology, Guangzhou 510080, People's Republic of China*

[d]*Department of Microbiology, School of Dental Medicine, University of Pennsylvania, Philadelphia, Pennsylvania 19104, USA*

† Electronic supplementary information (ESI) available: IR, MS, and 1D and 2D NMR data for compounds **1–13**. CCDC 1568169. For ESI and crystallographic data in CIF or other electronic format see DOI: 10.1039/c7ra08877a

‡ Shaonan Liu and Jiayuan Hu contributed equally.

Table 1 ^{1}H NMR chemical shifts (δ) of compounds **1–9** in $CDCl_3$ (400 MHz)

Position	1	2	3	4	5	6	7	8	9
1	2.43, m	2.24, m	1.92, m	2.10, m		2.35, m			4.50, t (3.0)
	2.32, m	1.99, m							
2	2.45, m	1.88, m	1.75, m	1.84, m	2.69, dd (17.6, 5.5)	1.81, m	2.79, dd (17.8, 5.2)	2.96, dd (17.3, 4.7)	1.94, m
		1.71, m	1.60, m		2.42, dd (17.6, 11.3)	1.64, m	2.52, dd (17.8,11.0)	2.46, dd (17.3, 8.2)	1.76, m
3		3.81, d (8.7)	3.89, d (12.5)	3.66, t (7.3)	3.81, dd (11.3, 5.5)	3.41, dd (11.6, 3.2)	3.83, dd (11.0, 5.2)	3.88, dd (8.2, 4.7)	3.89, dd (3.2, 12.9)
6	2.06, m	2.10, m	2.07, m	2.09, m	2.35, m			4.38, dd (4.2, 1.6)	
		1.95, m	1.92, m	1.99, m					
7	1.42, m	1.36, m	1.38, m	1.33, m	1.36, m	2.17, m	2.24, m	1.68, m	2.23, m
	1.33, m		1.32, m					1.39, m	
8	1.54, m	1.57, m	1.53, m	1.57, m	1.47, m	2.08, m	2.07, m	1.91, m	2.19, m
11	1.61, m	1.62, m	1.58, m	1.57, m	2.53, m	1.69, m	2.47, m	2.50, m	1.72, m
	1.30, m	1.37, m	1.30, m	1.28, m	1.12, m	1.51, m	1.25, m		2.00, m
12	1.54, m	1.53, m	1.53, m	1.57, m	1.61, m	1.57, m	1.64, m	1.64, m	1.40, m
	1.25, m	1.29, m	1.27, m	1.28, m	1.23, m	1.35, m	1.31, m	1.28, m	1.61, m
14	1.38, m	1.36, m	1.40, m	1.39, m	1.47, m	1.40, m	1.45, t (13.2)	1.53, m	1.18, m
	1.08, m	1.06, m	1.06, m	1.06, m	1.09, m	1.13, m	1.05, m	1.10, m	1.37, m
15	5.79, dd (17.5, 10.7)	5.80, dd (17.5, 10.7)	5.81, dd (17.5, 10.7)	5.81, dd (17.5, 10.7)	5.82, dd (17.5, 10.7)	5.80, dd (17.5, 10.7)	5.80, dd (17.5, 10.7)	5.83, dd (17.5, 10.7)	5.81, dd (17.5, 10.7)
16	4.90, d (17.5)	4.91, d (17.5)	4.91, d (17.5)	4.91, d (17.5)	4.93, d (17.5)	4.93, d (17.5, 1.3)	4.90, d (17.5)	4.94, d (17.5, 1.3)	4.95, d (17.5, 1.2)
	4.82, d (10.7)	4.83, d (10.7)	4.84, d (10.7)	4.84, d (10.7)	4.85, d (10.7)	4.87, d (10.7, 1.3)	4.82, d (10.7)	4.86, d (10.7, 1.3)	4.90, d (10.7, 1.2)
17	1.00, s	1.01, s	1.01, s	1.02, s	1.02, s	1.04, s	1.37, s	1.06, s	1.06, s
18	1.04, s	1.02, s	3.76, d (10.4)	1.16, s	1.21, s	1.21, s	1.29, s	1.41, s	1.15, s
			3.59, d (10.4)						
19	3.59, d (11.0)	3.56, d (10.9)	1.01, s	3.79, d (11.3)	1.07, s	1.29, s	1.04, s	1.19, s	1.35, s
	3.65, d (11.0)	3.51, d (10.9)		3.53, d (11.3)					
20	0.91, s	0.87, s	0.85, s	0.86, s	1.07, s	0.99, s	1.19, s	1.04, s	0.99, s

H-8/H_3-17, H-12a/H-15, and H-12a/H_3-20 indicated an α-orientation of CH_3-20 and β-orientations for H-8 and CH_3-17. The absolute configuration of compound **1** was determined as 4*R*, 8*S*, 9*S*, and 13*S* by single crystal X-ray crystallographic diffraction analysis of its *p*-bromobenzoate derivative **1a** with Cu Kα radiation (Fig. 2). Thus, the absolute configuration of compound **1** was defined as 4*R*, 8*S*, 9*S*, and 13*S*, and given the trivial name euphominoid A.

Compounds **2** (euphominoid B) and **3** (euphominoid C) were isolated using a chiral RP-HPLC column and had the same molecular formula of $C_{20}H_{32}O_2$. As shown in Table 1, the carbonyl signal at δ_C 216.5 in compound **1** was absent, while an oxygenated methine signal was observed at δ_C 72.4 for compound **2** and δ_C 73.2 for compound **3**. These observations suggested the presence of a hydroxy group at C-3 in both compounds **2** and **3**. For compound **2**, the HMBC cross-peaks between H_3-18 (δ_H 1.02, s)/H-19 (δ_H 3.56, d, J = 10.9 Hz; 3.51, d, J = 10.9 Hz) and the oxygenated methine carbon at δ_C 72.4 indicated that the hydroxy group was positioned at C-3. The corresponding cross-peaks observed in the HMBC spectrum obtained for compound **3** suggested similar results (Fig. S23, ESI†). By analysis of the NOESY spectra of compounds **2** and **3** (Fig. S16 and S24, ESI†), the cross-peaks of H-3/H_3-18 in compound **2** and the cross-peaks of H-3/H_3-19 in compound **3** revealed a *cis*-1,3-diol unit in **2** and **3**. Thus, the relative configuration of compounds **2** and **3** were established as shown.

The molecular formula of compound **4** (euphominoid D) was identified as $C_{20}H_{30}O$ from a protonated molecule at *m*/*z* 287.2355 $[M + H]^+$ in the HRESIMS data, which indicated the loss of a water molecule from compounds **2** or **3**. The NMR data of compound **4** were similar to those of compound **2** (Tables 1 and 2), except for a significant difference in the chemical shift of C-3 (δ_C 77.6 in compound **4** *vs.* 72.4 in compound **2**). The downfield C-3 in **4** indicated the formation of an oxygen bridge between C-3 and C-19.[20,21] The cross-peaks of H-3/H_3-18 in the NOESY spectrum of compound **4** (Fig. S32, ESI†) indicated the same orientations of H-3 and CH_3-18. Thus, the relative configuration of compound **4** was established as shown.

Biogenetically, compounds **2**, **3**, and **4** should possess the same absolute configurations as compound **1** at C-8, C-9, and C-13. Owing to the presence of the $\Delta^{5,10}$ double bond, no NOESY cross-peaks of H-3, H_3-18, or H-19 with H-8, H_3-17, or H_3-20 were observed for compounds **2**, **3**, and **4**. The absolute configurations of C-3 and C-4 in compounds **2**, **3**, and **4** could not be determined by comparison with those of compound **1**. Thus chemical transformations (Fig. 3) were used to establish the absolute configurations at C-3 and C-4 for compounds **2** and **4**. Compound **1** was reacted with $NaBH_4$ in MeOH to yield compounds **2** and **4** in yields of 58 and 8%. Thus, the 3*R*

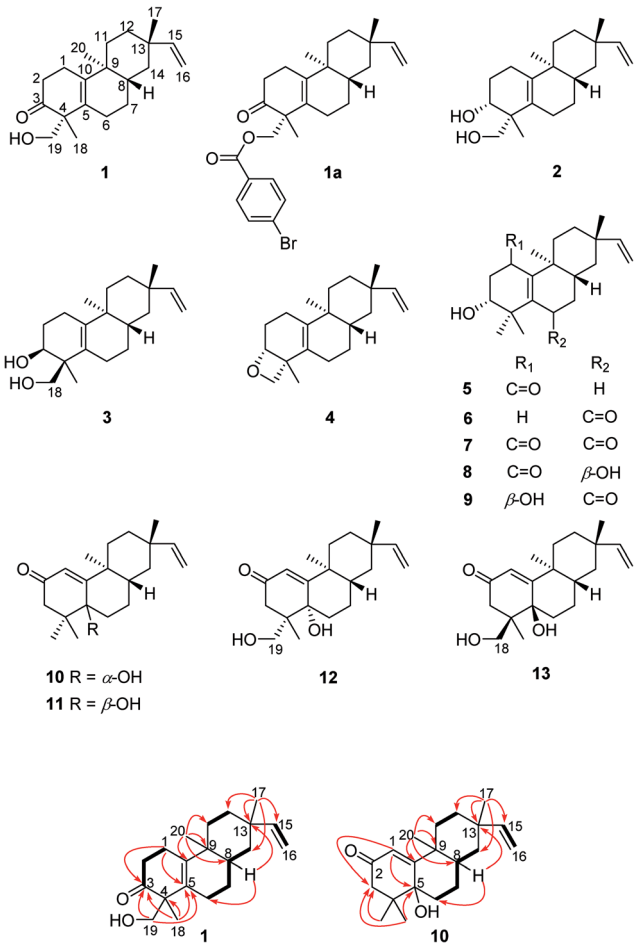

Fig. 1 Key $^{1}H-^{1}H$ COSY (▬) and HMBC (⟶) cross-peaks of compounds **1** and **10**.

absolute configurations in compounds **2** and **4** were defined through a combination of the 4*R* absolute configuration in compound **1** and the NOESY cross-peaks observed in compounds **2** and **4**. The absolute configurations of compounds **2** and **4** were assigned as 3*R*, 4*R*, 8*S*, 9*S*, and 13*S*.

Induced electronic circular dichroism spectrum (IECD) by $[Mo_2(OAc)_4]$ was used to define the absolute configuration of the *cis*-1,3-diol unit.[22,23] For the "semi-rigid" 1,3-diol moiety, only the *syn*-parallel orientation of the hydroxy groups allows for the formation a chiral complex with $Mo_2(OAc)_4$ leading to the Cotton effect (CE). The observed signal of the CE at 400 nm in the complex depends on the chirality of the 1,3-diol moiety. The strong positive CE band observed around 350 nm and a relatively weak negative CE band at 400 nm (Fig. 4) in the IECD spectra of compound **3** indicated that 3-OH and 18-CH_2OH are co-facial. On the basis of the empirical sector rule for 1,3-diols, the negative CE at 400 nm observed in the IECD spectra of compound **3** and the sector rule (Fig. 4) indicated a 3*S* and 4*S* absolute configurations for compound **3**. According to compound **1**, the absolute configuration of compound **3** was assigned as 3*S*, 4*S*, 8*S*, 9*S*, and 13*S*.

Compound **5** (euphominoid E), was obtained as a colorless gum with a molecular formula of $C_{20}H_{30}O_3$ based on the HRESIMS ion at *m*/*z* 301.2167 $[M - H]^-$. A UV absorption maximum at 246 nm and IR signals at 1636 and 1579 cm^{-1}, in combination with the observed ^{13}C NMR chemical shifts of δ_C 196.5, 162.2, and 142.3 suggested the presence of an α,β-unsaturated carbonyl group. Detailed analysis of the 1D and 2D NMR data of compound **5** (Fig. S35–S40, ESI†) revealed an *ent*-rosane diterpenoid similar to compound **1**. The HMBC cross-peaks from H_3-18 (δ_H 1.21)/H_3-19 (δ_H 1.07) to C-3 (δ_C 72.7), C-4 (δ_C 41.8), and C-5 (δ_C 162.2), and H_3-20 (δ_H 1.07) to C-10 (δ_C 142.3) suggested the presence of a $\Delta^{5,10}$ double bond and a hydroxy group at C-3

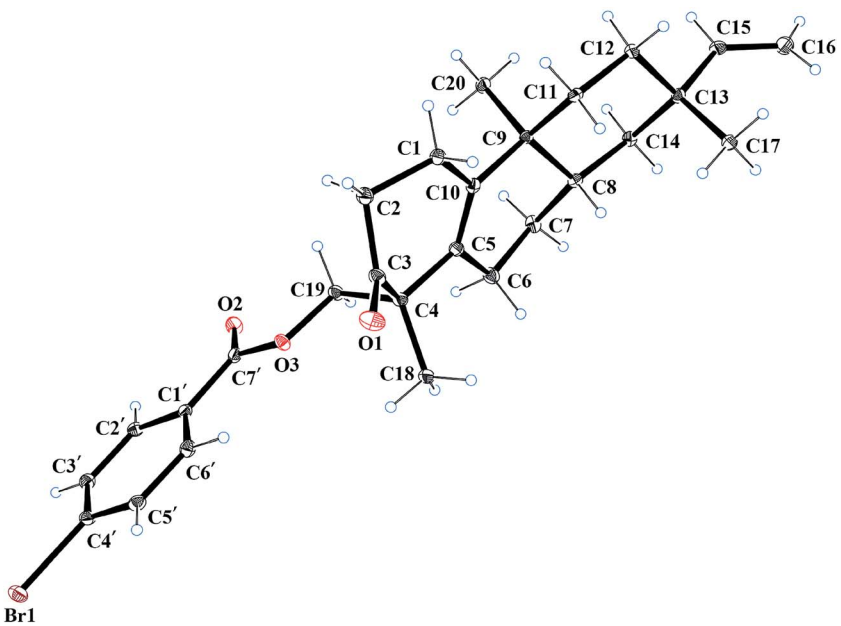

Fig. 2 X-ray ORTEP plot of the molecular structure of compound **1a**.

Table 2 ^{13}C NMR chemical shifts (δ) of compounds **1–9** in $CDCl_3$ (100 MHz)

Position	1	2	3	4	5	6	7	8	9
1	23.4	21.5	25.4	23.6	196.5	25.7	198.5	198.1	64.7
2	38.6	26.6	27.4	28.0	44.2	26.3	43.8	44.7	36.5
3	216.5	72.4	73.2	77.6	72.7	76.2	73.3	75.1	71.3
4	53.0	44.1	44.3	43.1	41.8	39.1	39.6	44.2	39.4
5	129.7	127.8	129.0	128.2	162.2	138.0	151.5	157.2	140.4
6	24.7	24.8	25.7	25.7	28.2	198.0	200.0	65.3	199.0
7	25.2	25.8	24.6	25.8	25.0	42.6	42.6	35.2	42.9
8	37.2	37.1	37.7	37.5	38.4	36.2	36.5	32.6	35.9
9	36.3	37.6	37.7	37.7	37.2	39.1	38.0	38.2	39.0
10	141.3	140.9	140.0	140.2	142.3	168.0	155.3	143.7	160.8
11	31.5	32.3	31.8	32.0	31.4	31.2	30.9	31.0	30.9
12	32.3	32.8	32.7	32.8	32.8	32.3	32.3	32.8	32.3
13	37.6	36.5	36.5	36.6	36.4	36.0	35.9	36.4	36.1
14	39.2	39.8	39.6	39.7	39.0	38.5	37.9	38.7	38.9
15	150.8	151.3	151.3	151.3	151.3	150.3	150.3	151.0	150.3
16	108.7	108.9	108.8	108.9	108.9	109.7	109.0	109.1	109.6
17	22.9	23.1	23.2	23.2	23.4	22.8	22.4	23.5	22.9
18	18.8	17.2	68.9	20.0	23.9	19.3	24.4	26.4	17.7
19	67.3	69.2	15.7	67.3	19.7	25.1	19.0	22.4	24.8
20	16.9	18.2	17.1	17.8	16.7	15.8	15.2	15.8	17.3

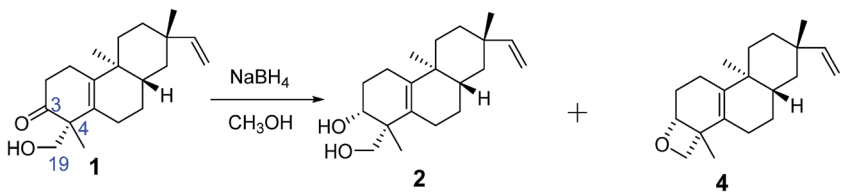

Fig. 3 Chemical transformation of compounds **1**, **2**, and **4**.

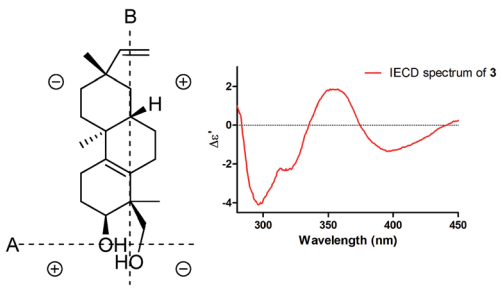

Fig. 4 Sector rule (left) and IECD (right) of compound **3**.

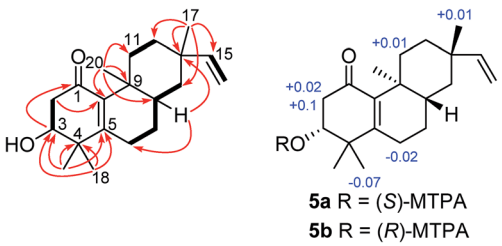

Fig. 5 $\Delta\delta_{S-R}$ values of MTPA esters of compound **5**.

(Fig. 5). A carbonyl group at C-1 was deduced from the HMBC cross-peak between H-3 and C-1 (Fig. 5). The absolute configuration of C-3 was determined using the Mosher's ester method.[17] Treatment of compound **5** with (*R*)- or (*S*)-MTPA chloride in anhydrous dichloromethane, 4-dimethylaminopyridine, and triethylamine yielded the (*S*)- and (*R*)-MTPA ester derivatives, respectively. The ^{1}H NMR chemical shift differences ($\Delta\delta_{S-R}$) between the 3*R* and 3*S* esters are shown in Fig. 5. The negative $\Delta\delta_{S-R}$ values for H-6 and H_3-18, and the positive values for H-2a, H-2b, and H-11a indicated the *R* configuration at C-3. In line with compound **1**, the absolute configuration of compound **5** was determined as 3*R*, 8*S*, 9*S*, and 13*S*.

The molecular formula of compound **6** (euphominoid F) was established as $C_{20}H_{30}O_2$ based on the HRESIMS ion at *m*/*z* 303.2312 $[M + H]^+$. The NMR data for this compound were similar to those of compound **5** (Tables 1 and 2), with the exception of the location of the carbonyl carbon. The carbonyl group at C-6 in compound **6** was deduced from the COSY cross-peaks of H-1 (δ_H 2.35, m)/H-2 (δ_H 1.81, m; 1.64, m) and H-2 (δ_H 1.81, m; 1.64, m)/H-3 (δ_H 3.41, dd, J = 11.6, 3.2 Hz), as well as an HMBC cross-peak between H-8 (δ_H 2.08, m) and C-6 (δ_C 198.0). The 2D structure of compound **6** was thus assigned as shown. Owing to the limited quantity obtained for compound **6**, the computed ECD method was employed to determine its absolute configuration. The ECD spectra were calculated using the Gaussian 09 program at the TD-DFT-PBE1PBE/6-31++G(2d,2p) level in MeOH. This calculation for the 3*R* configuration was in good agreement with the experimental ECD data (Fig. 6). Thus,

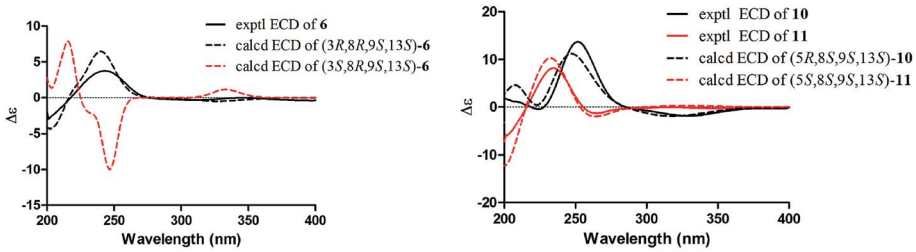

Fig. 6 Calculated and experimental ECD spectra of compounds **6**, **10** and **11**. The calculated ECD spectra were computed at the PBE1PBE/6-31++G(2d,2p) level in MeOH.

the absolute configuration of compound **6** was assigned as 3*R*, 8*R*, 9*S*, and 13*S*.

Compound **7** (euphominoid G) was found to have a molecular formula of $C_{20}H_{28}O_3$ based on the HRESIMS (*m*/*z* 315.1954 $[M - H]^-$). The structure of **7** was similar to compound **6**, except for an additional carbonyl group at C-1, which was supported by the HMBC cross-peaks between H-3 (δ_H 3.83, dd, J = 11.0, 5.2 Hz) and C-1 (δ_C 198.5). Detailed analysis of the 2D NMR data (Fig. S53–S56, ESI†) confirmed the 2D structure of compound **7**, and its absolute configuration was defined as 3*R*, 8*R*, 9*S*, and 13*S* through comparison of the calculated and experimental ECD data.

Compound **8** (euphominoid H) had the molecular formula $C_{20}H_{30}O_3$ (HRESIMS). The NMR data (Tables 1 and 2) suggested a structure similar to that of compound **7**. The HMBC cross-peaks of H-6 (δ_H 4.38, dd, J = 4.2, 1.6 Hz) with C-4 (δ_C 44.2), C-5 (δ_C 157.2), and C-8 (δ_C 32.6) indicated a hydroxy group at C-6 in compound **8**. In the NOESY spectrum (Fig. S64, ESI†), the cross-peaks between H-6 and H_3-20 suggested that H-6 and CH_3-20 were co-facial and assigned as α-orientations. According to compound **7**, the absolute configuration of compound **8** was defined as 3*R*, 6*R*, 8*R*, 9*S*, and 13*S*, which was confirmed by comparing the calculated and experimental ECD data.

Compound **9** (euphominoid I) was obtained as a colorless gum with a molecular formula of $C_{20}H_{30}O_3$ based on the HRESIMS ion at *m*/*z* 319.2264 $[M + H]^+$. Analysis of the 1D and 2D NMR data of compound **9** (Fig. S67–S72, ESI†) indicated a similar chemical structure to that of compound **8**. The CHO–CH_2–CHO fragment was deduced from the COSY cross-peaks of H-1 (δ_H 4.50, t, J = 3.0 Hz)/H-2 (δ_H 1.94, m; 1.76, m) and H-2 (δ_H 1.94, m; 1.76, m)/H-3 (δ_H 3.89, dd, J = 12.9, 3.2 Hz). The presence of a carbonyl group at C-6 was consistent with the HMBC cross-peaks of H-8/H-7 with C-6. In the NOESY spectrum (Fig. S72, ESI†), the cross-peaks of H-1/H_3-20 indicated that the 1-OH group was β-oriented. Since there were insufficient signals observed in the NOESY spectrum attributed to H-3, comparison of its experimental and calculated ECD was used to identify the configuration of C-3 (Fig. S105, ESI†). Thus, according to compound **8**, the absolute configuration of compound **9** was defined as 1*R*, 3*R*, 8*R*, 9*S*, and 13*S*.

Compound **10** (euphominoid J) was obtained as a colorless gum, and its molecular formula was determined as $C_{20}H_{30}O_2$ from the HRESIMS ion at *m*/*z* 303.2307 $[M + H]^+$. The NMR data of **10** (Table 3) were similar to those of ebractenoid J,[24] except for an additional methyl group and the absence of a cyclopropyl ring. The HMBC cross-peaks from H_3-18 (δ_H 1.06, s)/H_3-19 (δ_H 1.02, s) to C-3 (δ_C 48.5), C-4 (δ_C 40.9), and C-5 (δ_C 75.0) indicated two methyl groups positioned at C-4 and a hydroxy group at C-5.

Interestingly, compound **11** (5-*epi*-euphominoid J), the C-5 epimer of **10**, was also isolated. The ^{1}H NMR spectra of compounds **10** and **11** were closely comparable, with an evident difference observed in the chemical shift of H-8 (δ_H 1.47 in compound **10** *vs.* 2.25 in compound **11**), C-6 (δ_C 32.6 in compound **10** *vs.* 23.2 in compound **11**), and C-8 (δ_C 32.6 in compound **10** *vs.* 23.2 in compound **11**). Steric interactions existing between protons and their neighboring groups would result in a van-der-Waals effect that might lead to the deshielding of the protons.[25] Thus, comparison of the 3D structures of compounds **10** and **11** indicated the existence of the van-der-Waals effect between 5β-OH and 8β-H in compound **11** (Fig. 7). The ^{1}H NMR spectrum showed a discernible low field shift of the H-8 signal (δ_H 1.47 in compound **10** *vs.* 2.25 in compound **11**), which indicated that the 5-OH in compound **11** is β-oriented whereas in compound **10** this hydroxyl group is α-oriented. The distance between the 5-OH and H-8 groups was calculated using the TDDFT method at the M06-2X/6-31+G(d,p) level. As shown in Fig. 7, the distance between these two groups in compound **11** was found to be smaller than that in compound **10**. Thus, the absolute configuration of **10** was defined as 5*R*, 8*S*, 9*S*, and 13*S*, and compound **11** as 5*S*, 8*S*, 9*S*, and 13*S*, both of which were further confirmed by comparison of the experimental and calculated ECD spectra (Fig. 6).

Compound **12** (euphominoid K) had the molecular formula $C_{20}H_{30}O_3$ based on the HRESIMS ion at *m*/*z* 317.2117 $[M - H]^-$. The NMR data of compound **12** (Table 3) were similar to those of compound **10**, except for a methyl group in compound **10** being replaced by a hydroxymethyl group (δ_C 69.3). The HMBC cross-peaks of H-19 (δ_H 4.06, d, J = 11.5 Hz; 3.35, d, J = 11.5 Hz) with C-3 (δ_C 44.0), C-4 (δ_C 43.4), C-5 (δ_C 76.8), and C-18 (δ_C 21.4) suggested that the hydroxymethyl group is located at C-4. The 5-OH group was found to be α-oriented based on comparison of the chemical shift of H-8 with that of compounds **10** and **11** (Table 3). Taking into consideration the van-der-Waals effect induced by the 5-OH, as well as comparison of the chemical shifts of H-6a (δ_H 2.09, m) and H-6b (δ_H 1.83, m), it was suggested that the H-6a and 5-OH groups are co-facial. The NOESY cross-peak of H-19/H-6a (Fig. S96, ESI†) revealed that the 19-CH_2OH group was α-oriented. Thus, the absolute configuration

Table 3 ^{1}H (400 MHz) and ^{13}C (100 MHz) NMR chemical shifts (δ) of compounds **10–13** in $CDCl_3$

	10		**11**		**12**		**13**	
Position	δ_H (J in Hz)	δ_C	δ_H (J in Hz)	δ_C	δ_H (J in Hz)	δ_C	δ_H (J in Hz)	δ_C
1	5.95, s	123.7	5.93, s	123.2	5.98, s	123.9	5.95, s	123.4
2		200.5		200.7		200.8		201.2
3	2.73, d (16.4)	48.5	2.85, d (16.8)	48.6	3.33, d (16.3)	44.0	3.36, d (16.9)	43.9
	1.93, d(16.4)		2.00, d (16.8)		2.00, d (16.3)		1.97, d (16.9)	
4		40.9		41.3		43.4		43.9
5		75.0		74.6		76.8		76.3
6	1.92, m	32.6	1.88, m	23.2	2.09, m	33.1	2.04, m	23.9
	1.82, m		1.27, m		1.83, m		1.88, m	
7	1.25, m	24.3	1.88, m	22.9	1.83, m	24.2	1.87, m	23.0
			1.77, m		1.30, m		1.29, m	
8	1.47, m	38.8	2.25, m	29.7	1.48, m	38.5	2.21, m	29.6
9		40.0		38.3		40.0		38.2
10		169.3		171.6		168.8		171.1
11	1.71, m	32.9	1.78, m	34.2	1.73, m	32.8	1.78, m	34.1
	1.53, m		1.57, m		1.53, m		1.57, m	
12	1.63, m	32.3	1.57, m	32.7	1.64, m	32.2	1.57, m	32.6
	1.36, m		1.36, m		1.37, m		1.36, m	
13		36.2		36.3		36.2		36.2
14	1.47, m	39.4	1.27, m	40.1	1.48, m	39.4	1.25, m	40.1
	1.13, m				1.15, m		2.21, m	
15	5.81, dd (17.5, 10.7)	150.6	5.81, dd (17.5, 10.7)	150.7	5.82, dd (17.5, 10.7)	150.6	5.81, dd (17.5, 10.7)	150.7
16	4.94, dd (17.5, 1.0)	109.0	4.93, dd (17.5, 1.2)	109.4	4.94, dd (17.5, 1.3)	109.4	4.95, dd (17.5, 1.3)	109.3
	4.87, dd (10.7, 1.0)		4.87, dd (10.7, 1.2)		4.88, dd (10.7, 1.3)		4.88, dd (10.7, 1.3)	
17	1.01, s	22.9	0.99, s	22.5	1.02, s	22.9	1.00, s	22.4
18	1.06, s	25.4	1.09, s	24.9	0.87, s	21.4	4.05, d (11.4)	69.3
							3.38, d (11.4)	
19	1.02, s	23.4	0.97, s	23.5	4.06, d (11.5)	69.3	0.82, s	20.9
					3.35, d (11.5)			
20	1.21, s	19.2	1.09, s	17.5	1.20, s	19.6	1.00, s	18.7

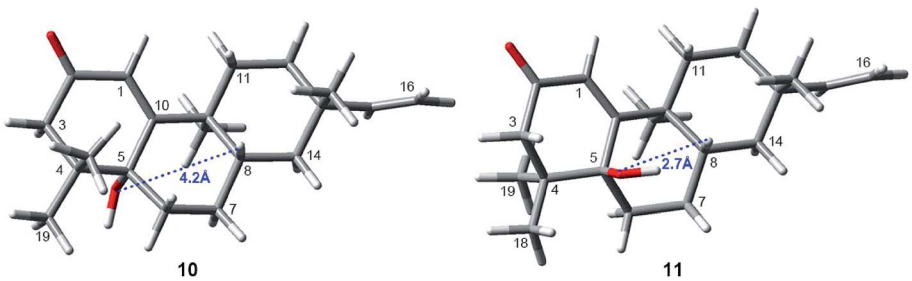

Fig. 7 The distance between the 5-OH and 8-H groups within compounds **10** and **11**. The calculated distance were computed at the M06-2X/6-31+G(d,p) level.

of compound **12** was defined as 4*S*, 5*S*, 8*S*, 9*S*, and 13*S*, which was further confirmed by comparison of its experimental and calculated ECD spectra (Fig. S106, ESI†).

Compound **13** (euphominoid L) had the same molecular formula as that of compound **12**, as well as similar ^{1}H NMR data, with evident differences in the chemical shifts of H-8. Given that the chemical shifts of H-8 in compounds **13** and **11** were almost identical, and also taking into account the van-der-Waals effect, the 5-OH group in compound **13** was suggested to be β-oriented, as in compound **11**. Therefore, the H-6a and 5-OH should be co-facial and have the same β-orientation. In the NOESY spectrum (Fig. S104, ESI†), the cross-peaks of H-18/H-6a indicated that the 18-CH_2OH group was β-oriented. Thus, the absolute configuration of compound **13** was identified as 4*R*, 5*R*, 8*S*, 9*S*, and 13*S*.

Compounds **1–13** were evaluated for their potencies in the inhibition of EBV lytic DNA replication in P3HR-1 cells using previous methods.[17,18] The tested compounds were initially assayed at 50 μM and (+)-rutamarin was used as a positive control.[26] Compounds **1–3** and **10** exhibited greater than 50% inhibition of EBV DNA lytic replication at 50 μM. These four compounds were then subjected to further tests to determine

Table 4 Anti-EBV lytic replication activities of the isolates from *E. milii*

Compound	EC_{50}[a]	R^{2d}	CC_{50}[b]	R^{2d}	SI[c]
1	13.2	0.9008	59.6	0.7798	4.5
2	5.4	0.9711	>50	0.8413	>9.3
3	24.4	0.8706	113	0.7707	4.6
10	29.1	0.9121	>200	0.7273	>6.9
(+)-Rutamarin[e]	5.4	0.879	>150	—	>39.6

[a] Inhibitory effects of the compounds against EBV lytic replication were tested and expressed as EC_{50} values (μM). [b] Cytotoxicities were measured after 2 days of compound treatment and expressed as CC_{50} values (μM). [c] Selective index (SI) = CC_{50}/EC_{50}. [d] Regression coefficients of the dose–response curves. [e] Positive control.

their half-maximal antiviral effective concentration (EC_{50}), half-maximal cytotoxic concentration (CC_{50}), and selective index (SI) values (Table 4).

Conclusions

Thirteen new *ent*-rosane diterpenoids were isolated from the air parts of *E. milii*. Four compounds **1–3** and **10** showed moderate inhibitory activity of EBV DNA lytic replication. Compound **2** exhibited significant inhibitory activity with EC_{50} values of 5.4 μM. Based on these results, preliminary SAR (structure–activity relationship) effects could be established. Thus, structurally, the 13 compounds tested were divided into two groups: in group 1, all of the compounds (**1–4**) possessed a $\Delta^{5,10}$ double bond, while the compounds in group 2 (**5–13**) contained an α,β-unsaturated carbonyl group. As shown in Table 4, compounds **1–3** showed medium to potent activity with EC_{50} values of 13.2, 5.4, and 24.4 μM, respectively. While compounds **5–13** found to be inactive against EBV lytic replication, except compound **10** showed medium activity (EC_{50} = 29.1 μM). These results suggested that the isolated olefinic scaffolds exhibited significant inhibitory activity than the α,β-unsaturated carbonyl group scaffolds against EBV lytic replication.

Experimental section

General experimental procedures

Optical rotation was determined on a Perkin-Elmer 341 polarimeter. UV spectra were record on a Shimadzu UV2450 spectrophotometer. ECD data were collected on an Applied Photophysics Chirascan spectrometer. IR spectra were recorded from KBr pellets on a Bruker Tensor 37 infrared spectrophotometer. The ^1H and ^{13}C NMR spectra were measured on a Bruker AVANCE-400 NMR spectrometer operating at 400 MHz and 100 MHz, respectively, with TMS as the internal reference. The HRESIMS and ESIMS data were determined on a Shimadzu LCMS-IT-TOF mass spectrometer and an Agilent 1200 series LC-MS/MS system, respectively. Semipreparative chiral HPLC separation was carried out on an LC-20AT Shimadzu liquid chromatography system with a Phenomenex Lux cellulose-2 chiral-phase column (250 × 10 mm, 5 μm) and Agilent ZORBAX SB-C18 column (250 × 9.4 mm, 5 μm). X-ray data were collected using an Agilent Xcalibur (Onyx, Nova) diffractometer. TLC silica gel plates were purchased from Marine Chemical Ltd., Qingdao, People's Republic of China. RP_{18} reversed-phase silica gel (Fuji, 40-75 μm), MCI gel (CHP20P, 75-150 μm, Mitsubishi Chemical Corporation, Tokyo, Japan), silica gel (200–300 Mesh, Marine Chemical Ltd.), and Sephadex LH-20 (GE Healthcare Bio-Sciences AB, Uppsala, Sweden) were used for column chromatography (CC).

Plant material

The aerial parts of *E. milii* (3.0 kg) were collected in Baoshan District, Yunnan Province, People's Republic of China, on September 19, 2014, and identified by Dr Chunyan Han from the Kunming Institute of Botany, Chinese Academy of Sciences. A voucher specimen (XG-2014001) was deposited at the School of Pharmacy Sciences, Sun Yat-sen University.

Extraction and isolation

The air-dried aerial parts of *E. milii* (3.0 kg) was powdered and extracted with 80% acetone in water (3 × 20 L) at room temperature for 2 days. The solvent was removed under reduced pressure to give a crude extract (400 g), which was suspended in H_2O and extracted successively with EtOAc (3 × 3 L). The EtOAc-soluble fraction (180 g) was chromatographed over a silica gel column, eluting with a step gradient of cyclohexane–EtOAc to give fractions A–C. Partition B (50 g) was loaded onto a silica gel column and eluted with a gradient of CH_2Cl_2–EtOAc from 200 : 1 to afford six fractions (B1–B6). Fraction B2 was separated on a silica gel column, eluting with cyclohexane–EtOAc (40 : 1), and further purified by preparative HPLC using 80% CH_3CN–H_2O as the solvent to afford compounds **1** (500 mg) and **6** (4 mg). Compounds **10** (10 mg) and **11** (10 mg) were isolated from fraction B3 by semi-preparative HPLC, eluting with MeOH–H_2O (88 : 12). Fraction B4 (16 g) was loaded onto a silica gel column and eluted with cyclohexane–EtOAc (40 : 1) to afford subfractions B4a–B4c, which were sequentially purified by preparative HPLC, eluting with CH_3CN–H_2O (85%, 75%, and 65%) to afford compounds **2** (400 mg), **3** (15 mg), **4** (10 mg), **5** (4 mg), **7** (4 mg), **8** (6 mg), **9** (4 mg), **12** (8 mg), and **13** (14 mg).

Euphominoid A (1). White powder; $[\alpha]_D^{25}$ + 210 (*c* 0.2, MeOH); IR (KBr) ν_{max} 3408, 2922, 1695, 1639, 1377, 1047 cm^{-1}; ^1H NMR (400 MHz, $CDCl_3$) and ^{13}C NMR (100 MHz, $CDCl_3$) data, see Tables 1 and 2; HRESIMS *m*/*z* 325.2132 $[M + Na]^+$ (calcd for $C_{20}H_{30}O_2Na$, 325.2138).

Euphominoid B (2). White powder; $[\alpha]_D^{25}$ + 95 (*c* 0.1, MeOH); IR (KBr) ν_{max} 3332, 2927, 1639, 1375, 1033 cm^{-1}; ^1H NMR (400 MHz, $CDCl_3$) and ^{13}C NMR (100 MHz, $CDCl_3$) data, see Tables 1 and 2; HRESIMS *m*/*z* 327.2292 $[M + Na]^+$ (calcd for $C_{20}H_{32}O_2Na$, 327.2295).

Euphominoid C (3). White powder; $[\alpha]_D^{25}$ + 71 (*c* 0.2, MeOH); IR (KBr) ν_{max} 3428, 2933, 1262, 1089 cm^{-1}; ^1H NMR (400 MHz, $CDCl_3$) and ^{13}C NMR (100 MHz, $CDCl_3$) data, see Tables 1 and 2; HRESIMS *m*/*z* 303.2324 $[M - H]^-$ (calcd for $C_{20}H_{31}O_2$, 303.2330).

Euphominoid D (4). White powder; $[\alpha]_D^{25}$ + 96 (*c* 0.1, MeOH); IR (KBr) ν_{max} 3280, 2929, 1639, 1464, 1045 cm^{-1}; ^1H NMR (400 MHz, $CDCl_3$) and ^{13}C NMR (100 MHz, $CDCl_3$) data, see

Table 2; HRESIMS *m/z* 287.2355 $[M + H]^+$ (calcd for $C_{20}H_{31}O$, 287.2369).

Euphominoid E (5). Colorless gum; $[\alpha]_D^{25}$ + 85 (*c* 0.1, MeOH); UV (MeOH) λ_{max} (log ε) 247 (3.71) nm; ECD (MeOH) λ_{max} ($\Delta\varepsilon$) 246 (+7.72), 326 (−0.75) nm; IR (KBr) ν_{max} 3407, 2932, 1636, 1579, 1314 cm^{-1}; ^1H NMR (400 MHz, $CDCl_3$) and ^{13}C NMR (100 MHz, $CDCl_3$) data, see Tables 1 and 2; HRESIMS *m/z* 301.2167 $[M - H]^-$ (calcd for $C_{20}H_{29}O_2$, 301.2173).

Euphominoid F (6). Colorless gum; $[\alpha]_D^{25}$ + 88 (*c* 0.1, MeOH); UV (MeOH) λ_{max} (log ε) 248 (3.77) nm; ECD (MeOH) λ_{max} ($\Delta\varepsilon$) 244 (+3.74) nm; IR (KBr) ν_{max} 3446, 2928, 1644, 1582, 1372, 1067 cm^{-1}; ^1H NMR (400 MHz, $CDCl_3$) and ^{13}C NMR (100 MHz, $CDCl_3$) data, see Tables 1 and 2; HRESIMS *m/z* 303.2312 $[M + H]^+$ (calcd for $C_{20}H_{31}O_2$, 303.2319).

Euphominoid G (7). Colorless gum; $[\alpha]_D^{25}$ + 44 (*c* 0.1, MeOH); UV (MeOH) λ_{max} (log ε) 206 (3.22), 261 (3.55) nm; ECD (MeOH) λ_{max} ($\Delta\varepsilon$) 211 (−2.82), 262 (+3.33) nm; IR (KBr) ν_{max} 3390, 2922, 1677, 1656, 1465, 1051 cm^{-1}; ^1H NMR (400 MHz, $CDCl_3$) and ^{13}C NMR (100 MHz, $CDCl_3$) data, see Tables 1 and 2; HRESIMS *m/z* 315.1954 $[M - H]^-$ (calcd for $C_{20}H_{28}O_3Na$, 315.1966).

Euphominoid H (8). White powder; $[\alpha]_D^{25}$ + 33 (*c* 0.1, MeOH); UV (MeOH) λ_{max} (log ε) 204 (2.71), 244 (3.00) nm; ECD (MeOH) λ_{max} ($\Delta\varepsilon$) 202 (−1.19), 247 (+2.20), 232 (−0.57) nm; IR (KBr) ν_{max} 3394, 2924, 1651, 1464, 1044, 802 cm^{-1}; ^1H NMR (400 MHz, $CDCl_3$) and ^{13}C NMR (100 MHz, $CDCl_3$) data, see Tables 1 and 2; HRESIMS *m/z* 319.2276 $[M + H]^+$ (calcd for $C_{20}H_{31}O_3$, 319.2268).

Euphominoid I (9). Colorless gum; $[\alpha]_D^{25}$ + 36 (*c* 0.1, MeOH); UV (MeOH) λ_{max} (log ε) 203 (3.05), 244 (3.45) nm; ECD (MeOH) λ_{max} ($\Delta\varepsilon$) 204 (−0.50), 243 (+0.65), 352 (+0.36) nm; IR (KBr) ν_{max} 3390, 2923, 1650, 1380, 1044 cm^{-1}; ^1H NMR (400 MHz, $CDCl_3$) and ^{13}C NMR (100 MHz, $CDCl_3$) data, see Tables 1 and 2; HRESIMS *m/z* 319.2264 $[M + H]^+$ (calcd for $C_{20}H_{31}O_3$, 319.2268).

Euphominoid J (10). Colorless gum; $[\alpha]_D^{25}$ + 103 (*c* 0.1, MeOH); UV (MeOH) λ_{max} (log ε) 234 (4.03) nm; ECD (MeOH) λ_{max} ($\Delta\varepsilon$) 251 (+13.64), 330 (−1.89) nm; IR (KBr) ν_{max} 3483, 2968, 1664, 1610, 1317 cm^{-1}; ^1H NMR (400 MHz, $CDCl_3$) and ^{13}C NMR (100 MHz, $CDCl_3$) data, see Table 3; HRESIMS *m/z* 303.2307 $[M + H]^+$ (calcd for $C_{20}H_{31}O_2$, 303.2319).

5-*epi*-Euphominoid J (11). Colorless gum; $[\alpha]_D^{25}$ + 8 (*c* 0.2, MeOH); UV (MeOH) λ_{max} (log ε) 237 (3.98) nm; ECD (MeOH) λ_{max} ($\Delta\varepsilon$) 234 (+8.21), 265 (−1.31) nm; IR (KBr) ν_{max} 3387, 2936, 1655, 1611, 1467, 1316 cm^{-1}; ^1H NMR (400 MHz, $CDCl_3$) and ^{13}C NMR (100 MHz, $CDCl_3$) data, see Table 3; HRESIMS *m/z* 303.2308 $[M + H]^+$ (calcd for $C_{20}H_{31}O_2$, 303.2319).

Euphominoid K (12). White powder; $[\alpha]_D^{25}$ + 72 (*c* 0.1, MeOH); UV (MeOH) λ_{max} (log ε) 208 (3.74), 231 (3.79) nm; ECD (MeOH) λ_{max} ($\Delta\varepsilon$) 201 (+6.17), 248 (+4.87) nm; IR (KBr) ν_{max} 3427, 2964, 1657, 1094 cm^{-1}; ^1H NMR (400 MHz, $CDCl_3$) and ^{13}C NMR (100 MHz, $CDCl_3$) data, see Table 3; HRESIMS *m/z* 317.2117 $[M - H]^-$ (calcd for $C_{20}H_{29}O_3$, 319.2122).

Euphominoid L (13). White powder; $[\alpha]_D^{25}$ + 19 (*c* 0.1, MeOH); UV (MeOH) λ_{max} (log ε) 237 (3.79) nm; ECD (MeOH) λ_{max} ($\Delta\varepsilon$) 201 (−1.56), 222 (−1.24), 234 (+2.23) nm; IR (KBr) ν_{max} 3475, 2935, 1654, 1046 cm^{-1}; ^1H NMR (400 MHz, $CDCl_3$) and ^{13}C NMR (100 MHz, $CDCl_3$) data, see Table 3; HRESIMS *m/z* 317.2116 $[M - H]^-$ (calcd for $C_{20}H_{29}O_3$, 319.2122).

Preparation of the *p*-bromobenzoyl derivative of compound 1

To a stirred solution of compound **1** (50 mg, 0.16 mmol) in dry dichloromethane (10 mL) were added *p*-bromobenzoyl chloride (100 mg, 0.45 mmol), 4-dimethylaminopyridine (10 mg, 0.08 mmol), and trimethylamine (0.1 mL) at room temperature. When compound **1** was completely consumed (monitored by TLC), the reaction mixture was extracted with diluted hydrochloric acid and concentrated under reduced pressure to give a white solid residue, which was further purified by silica gel chromatography using dichloromethane as solvent to yield compound **1a** (60 mg, 77%). Compound **1a** was recrystallized from ethyl acetate as colorless crystals. ^1H NMR (400 MHz, $CDCl_3$): δ_H 7.78 (d, J = 8.4 Hz, 2H), 7.53 (d, J = 8.4 Hz, 2H), 5.80 (dd, J = 10.7, 17.5 Hz, 1H), 4.88 (m, 2H), 4.53 (d, J = 10.9 Hz, 1H), 4.35 (d, J = 10.9 Hz, 1H), 2.53 (m, 2H), 2.39 (m, 2H), 1.68–1.48 (m, 3H), 1.48–1.25 (m, 5H), 1.19 (s, 3H), 1.02 (s, 3H), 1.09 (m, 1H), 0.81 (s, 3H) ppm; ^{13}C NMR (100 MHz, $CDCl_3$): δ_C 213.7, 165.2, 151.0, 141.7, 131.9, 131.1, 129.3, 128.9, 128.3, 109.0, 68.8, 51.3, 39.4, 38.3, 38.0, 37.5, 36.5, 32.6, 31.8, 25.4, 23.6, 23.2, 19.3, 17.1 ppm.

X-ray crystallographic study of compound 1a

$C_{27}H_{33}BrO_3$, M = 485.46, monoclinic, 0.4 × 0.3 × 0.2 mm^3, space group $P2_1$, a = 5.86059 (7) Å, b = 12.67519 (17) Å, c = 15.73654 (19) Å, $\alpha = 90°$, $\beta = 94.4504\ (11)°$, $\gamma = 90°$, V = 1165.45 (3) $Å^3$, $Z = 2$, $D_{calc} = 1.3833$ g cm^{-3}, $F_{000} = 508.0$, Xcalibur, Onyx, Nova, Cu Kα radiation, λ = 1.54184 Å, T = 100 K, $2\theta_{max}$ = 144.24°, 21 844 reflections collected, 4565 unique ($R_{int} = 0.0358$). Final GooF = 1.035, $R_1 = 0.0257$, w$R_2 = 0.0704$, R indices based on 4565 reflections with $I > 2$ sigma(I) (refinement on F^2), 291 parameters, 1 restraint. Lp and absorption corrections applied, μ = 2.602 mm^{-1}. Flack parameter = 0.003 (10). Crystallographic data for the structure of **1a** have been deposited at the Cambridge Crystallographic Data Centre under the reference number CCDC 1568169.†

Conversion of 1 to 2 and 4

To a solution of **1** (50 mg, 0.17 mmol) in MeOH (5 mL), $NaBH_4$ (6.3 mg, 0.34 mmol) was added at 0 °C. The reaction was stirred for 10 h at room temperature until all starting material was consumed. The solvent was removed under reduced pressure. The residue was purified by preparative TLC (cyclohexane/EtOAc, 2/1) to afford compounds **2** (30 mg, 58% yield) and **4** (4 mg, 8% yield).

Determination of the absolute configuration of the *cis*-1,3-diol unit within compound 3

The IECD spectrum of compound **3** (0.50 mM in a $[Mo_2(OAc)_4]$ (0.10 mM) DMSO solution for 0 and 30 min) were measured on an Applied Photophysics Chirascan spectrometer in a 1 cm pathlength between 450 nm and 280 nm. The IECD spectrum of compound **3** was subtracted from the IECD spectrum of those complexes at 0 min, and the absolute configuration of the *cis*-1,3-diol moiety of compound **3** was assessed following sector rule. $[Mo_2(OAc)_4]$ (Strem) and DMSO (Sigma-Aldrich, anhydrous

≥99.9%) were commercially available and used without further purification.

Preparation of (*R*)- and (*S*)-MTPA esters of compound 5

To a solution of compound **5** (3 mg), 4-dimethylaminopyridine (DMAP, 10 mg) and triethylamine (0.025 mL) in anhydrous dichloromethane (1 mL) was added an excess of (*R*)- or (*S*)-MTPA chloride (20 μL), and the reaction was stirred for 1 h at room temperature. The reaction mixture was then purified by preparative silica gel TLC using cyclohexane–EtOAc (2 : 1) as the developing solvent.

^{1}H NMR data of (*R*)-MTPA ester of compound **5** (400 MHz, $CDCl_3$): δ_H 7.53–7.40 (5H, m, Ar–H), 5.82 (1H, dd, J = 10.7, 17.5 Hz, H-15), 5.17 (1H, dd, J = 5.6, 10.6 Hz, H-3), 4.93 (1H, dd, J = 1.4, 17.5 Hz, H-16a), 4.86 (1H, dd, J = 1.4, 10.7 Hz, H-16b), 2.88 (1H, dd, J = 5.6, 17.6 Hz, H-2a), 2.48 (1H, m, H-11a), 2.46 (1H, dd, J = 10.6, 17.6 Hz, H-2b), 2.34 (2H, m, H-6), 1.16 (3H, s, H-18), 1.07 (3H, s, H-19 or H-20), 1.04 (3H, s, H-20 or H-19), 1.02 (3H, s, H-17).

^{1}H NMR data of (*S*)-MTPA ester of compound **5** (400 MHz, $CDCl_3$): δ_H 7.53–7.40 (5H, m, Ar–H), 5.82 (1H, dd, J = 10.7, 17.5 Hz, H-15), 5.21 (1H, dd, J = 5.5, 10.5 Hz, H-3), 4.93 (1H, dd, J = 1.3, 17.5 Hz, H-16a), 4.86 (1H, dd, J = 1.3, 10.7 Hz, H-16b), 2.90 (1H, dd, J = 5.5, 17.5 Hz, H-2a), 2.56 (1H, dd, J = 10.5, 17.5 Hz, H-2b), 2.49 (1H, dt, J = 3.6, 13.3 Hz, H-11a), 2.32 (2H, m, H-6), 1.09 (3H, s, H-18), 1.06 (3H, s, H-19 or H-20), 1.04 (3H, s, H-20 or H-19), 1.03 (3H, s, H-17).

ECD computational calculations for compounds 5–13

The ECD spectra were calculated using Gaussian 09 and analyzed using the GUI GaussView (version 5.0) at the density functional theory (DFT) and time-dependent DFT (TD-DFT) levels. Conformational analysis of these compounds was performed using the Discovery Studio 3.5 (Accelrys Inc., San Diego, CA) software package. The minimum energy conformations were fully optimized at the B3LYP/6-31G(d) level in the gas phase to obtain accurate conformers. The ECD spectra were simulated at the PBE1PBE/6-31++G(2d,2p) level in MeOH. The calculated ECD curve was generated using SpecDis with σ = 0.2 eV.

Configuration computational calculations for compounds 10–13

The structures of compounds **10–13** were optimized at the M06-2X/6-31+G(d,p) in the gas phase using Gaussian 09. The distance between hydroxyl and H-8 was measured using Gaussian 09 and analyzed using GUIs GaussView (version 5.0), and the spectra were given in Fig. S155 and S156.†

Bioassay of extracts and compounds isolated from *E. milii* on the inhibition of EBV DNA lytic replication

The anti-EBV activities were assayed according to a method reported in the literature.[17,18] P3HR-1 cells were cultured in RPMI 1640 medium (Gibco-BRL, Gaithersburg, MD, USA) supplemented with 10% fetal bovine serum (Gibco-BRL), streptomycin (100 μg mL^{-1}), and penicillin (100 units per mL). The crude extracts and isolated compounds were dissolved in dimethyl sulfoxide (DMSO), and the final DMSO concentration in the culture medium was less than 0.5%. P3HR-1 cells were induced with 12-*O*-tetradecanoylphorbol-13-acetate (TPA) (20 ng mL^{-1}) and sodium butyrate (0.3 mM) for EBV lytic replication. After 3 h, the induced cells were treated with the extracts or compounds over varying concentrations. After 48 h, the P3HR-1 cells were harvested, and the total DNA in the cells was purified using the HiPure Tissue DNA Kit according to the manufacturer's protocol (Magen). The EBV genomic copy number was quantified by real-time PCR on a Roche 480 LightCycler using the LightCycler FastStart DNA Master^{Plus} SYBR Green Kit with primers for the detection of EBNA1 (sense: 5′-CATTGAGTCGTCTCCCCTTTGGAAT-3′; antisense: 5′-TCATAACAAGGTCCTTAATCGCATC-3′). The intracellular viral genomic DNA in each sample was normalized to GAPDH using the primers directed to GAPDH (sense: 5′-ACATCATCCCTGCCTCTAC-3′; antisense: 5′-TCAAAGGTGGAGGAGTGG-3′). The EC_{50} value of each compound was determined from a dose–response curve of the EBV DNA contents from TPA/butyrate-induced and compound-treated cells. The EC_{50} values for each compound were calculated according to previous methods[17,18] using GraphPad Prism software.

Cytotoxicity assays

The cell viability of P3HR-1 cells, after treatment with either the compounds or only DMSO, was tested by counting the trypan blue-stained cells using a light microscope after two days of treatment. The cell viability was defined relative to the control cells (non-drug-treated). The CC_{50} value was obtained from the dose–response curves using GraphPad Prism software.

Conflicts of interest

There are no conflicts to declare.

Acknowledgements

This study was supported in part by the Guangdong Province Frontier and Key Technology Innovation Program (2015B010109004), the College Key Training Program for Excellent Young Teacher (17ykzd13), the Guangdong Innovative Research Team Program (2009010058), and the National Natural Science Foundation of China (Nos. 81471138, 81573310, 81371793, 81530069).

References

1 Q. W. Shi, X. H. Su and H. Kiyota, *Chem. Rev.*, 2008, **108**, 4295–4327.
2 A. Vasas and J. Hohmann, *Chem. Rev.*, 2014, **114**, 8579–8612.
3 H. B. Wang, X. Y. Wang, L. P. Liu, G. W. Qin and T. G Kang, *Chem. Rev.*, 2015, **115**, 2975–3011.
4 A. Vasas, D. Rédei, D. Csupor, J. Molnár and J. Hohmann, *Eur. J. Org. Chem.*, 2012, **2012**, 5115–5130.

5 Y. Ito, M. Kawanishi, T. Harayama and S. Takabayashi, *Cancer Lett.*, 1981, **12**, 175–180.
6 C. M. Yang, H. Y. Cheng, T. C. Lin, L. C. Chiang and C. C. Lin, *Clin. Exp. Pharmacol. Physiol.*, 2005, **32**, 346–349.
7 L. Avila, M. Perez, G. Sanchez-Duffhues, R. Hernandez-Galan, E. Munoz, F. Cabezas, W. Quinones, F. Torres and F. Echeverri, *Phytochemistry*, 2010, **71**, 243–248.
8 R. J. Gulakowski, J. B. McMahon, R. W. Buckheit Jr, K. R. Gustafson and M. R. Boyd, *Antiviral Res.*, 1997, **33**, 87–97.
9 C. Jiang, P. Luo, Y. Zhao, J. Hong, S. L. Morris-Natschke, J. Xu, C. H. Chen, K. H. Lee and Q. Gu, *J. Nat. Prod.*, 2016, **79**, 578–583.
10 H. Y. Cheng, T. C. Lin, C. M. Yang, K. C. Wang, L. T. Lin and C. C. Lin, *J. Antimicrob. Chemother.*, 2004, **53**, 577–583.
11 I. Mucsi, J. Molnar, J. Hohmann and D. Redei, *Planta Med.*, 2001, **67**, 672–674.
12 T. Akihisa, E. M. Kithsiri Wijeratne, H. Tokuda, F. Enjo, M. Toriumi, Y. Kimura, K. Koike, T. Nikaido, Y. Tezuka and H. Nishino, *J. Nat. Prod.*, 2002, **65**, 158–162.
13 A. M. Madureira, J. R. Ascenso, L. Valdeira, A. Duarte, J. P. Frade, G. Freitas and M. J. Ferreira, *Nat. Prod. Res.*, 2003, **17**, 375–380.
14 M. J. Ahn, C. Y. Kim, J. S. Lee, T. G. Kim, S. H. Kim, C. K. Lee, B. B. Lee, C. G. Shin, H. Huh and J. Kim, *Planta Med.*, 2002, **68**, 457–459.
15 W. Li, X. Cai, Z. H. Hu and Y. J. Wang, *Chinese Wild Plant Resources*, 2008, **27**, 1–4.
16 S. N. Liu, D. Huang, S. L. Morris-Natschke, H. Ma, Z. H. Liu, N. P. Seeram, J. Xu, K. H. Lee and Q. Gu, *Org. Lett.*, 2016, **18**, 6132–6135.
17 H. Cui, B. Xu, T. Wu, J. Xu, Y. Yuan and Q. Gu, *J. Nat. Prod.*, 2014, **77**, 100–110.
18 T. Wu, Q. Wang, C. Jiang, S. L. Morris-Natschke, H. Cui, Y. Wang, Y. Yan, J. Xu, K. H. Lee and Q. Gu, *J. Nat. Prod.*, 2015, **78**, 500–509.
19 Y. Wang, L. Zhang, F. Wang, Z. H. Li, Z. J. Dong and J. K. Liu, *Nat. Prod. Bioprospect.*, 2015, **5**, 69–75.
20 I. Jantan and P. G. Waterman, *Phytochemistry*, 1994, **37**(5), 1477–1479.
21 L. Anwar, E. Mai, M. Ninomiya, S. Ibrahim, D. P. Putra, K. Tanaka and M. Koketsu, *Med. Chem. Res.*, 2017, DOI: 10.1007/s00044-017-1937-3.
22 J. Frelek, G. Snatzke and W. J. Szczepek, *Fresenius. J. Anal. Chem.*, 1993, **345**, 683–687.
23 J. Frelek, W. Szczepek and W. Voelter, *J. Prakt. Chem.*, 1997, **339**, 135–139.
24 Z. G. Liu, Z. L. Li, J. Bai, D. L. Meng, N. Li, Y. H. Pei, F. Zhao and H. M. Hua, *J. Nat. Prod.*, 2014, **77**, 792–799.
25 H. Günther, *NMR Spectroscopy: Basic Principles, Concepts and Applications in Chemistry*, Wiley-VCH, Germany, 3rd edn, 2013.
26 T. Wu, Y. Wang and Y. Yuan, *Antiviral Res.*, 2014, **107**, 95–101.